Arch. Metall. Mater. **68** (2023), 1, 171-185

DOI: https://doi.org/10.24425/amm.2023.141491

B. GOBALAKRISHNAN[1*], C. RAJARAVI[2], GOBIKRISHNAN UDHAYAKUMAR[3], P.R. LAKSHMINARAYANAN[4]

A COMPARATIVE STUDY ON EX-SITU & IN-SITU FORMED METAL MATRIX COMPOSITES

An attempt has been made to synthesize the aluminium based ex-situ (Al-SiC) and in-situ (Al-TiB_2) formed metal matrix composites with varying weight percentage of reinforcement contents such as 4wt.%, 6wt.% and 8wt.%. Synthesized composites were subjected to a cold extrusion process followed by heat treatment according to the ASTM B 918-01 standards. The mechanical properties of in-situ composites were evaluated as per the ASTM guidelines and compared with ex-situ formed composites and base metal properties. Superior properties were noticed in the in-situ formed composites and the mechanical properties such as yield strength, Ultimate tensile strength (UTS) and Hardness for both ex-situ and in-situ composites were found to increase with increasing the reinforcement addition. Cold extruded Al-8 wt.% SiC composite properties such as hardness, yield strength and UTS are 87 R_B, 152 MPa, 216 MPa respectively. Whereas, for Al-8 wt.% TiB_2 composite, the corresponding properties are 94 R_B, 192 MPa, 293 MPa. The morphology of the composites is analysed by Optical and Scanning Electron Microscopic (SEM) whereas presence of reinforcement particles such SiC and TiB_2 along with intermetallic phases Mg_2Si and Al_5FeSi are confirmed by EDX, XRD and Element Mapping analyses.

Keywords: MMCs; Al-SiC; Al-TiB_2; Extrusion; Heat treatment; Mechanical properties; Microstructure

1. Introduction

Aluminium metal matrix composites (AMMCs) are widely used materials, due to the fact that they have the potential for current demands of pioneering engineering applications [1,2]. Because of its high specific strength, superior formability and corrosion resistance, aluminium and its alloys are widely employed in numerous industries such as aerospace, transportation, and a variety of structural applications [1,3]. Porosity, bigger grain size, particle clustering, poor bonding, poor wetting, and unfavourable interfacial reaction product are common issues of AMMCs manufactured using the classical ex-situ technique, in which externally prepared reinforcements are put into the matrix material [1-4]. The wettability of ceramic particulates is one of the major criteria to achieve good interfacial bonding between the matrix and reinforcement phases. Though most of the ceramic particles i.e., SiC, Al_2O_3 are not wetted by the aluminium melt and hence it is difficult to obtain uniform dispersion of reinforcement particles throughout the aluminium matrix. Contact angle is one of the significate factors for the wettability of the composite. Wettability was enhanced with decreasing the contact angle between Al and ceramic reinforcements [5,6]. In other words, contact angles between ceramic particles (SiC, Al_2O_3, graphite) and molten aluminium are important factors for the wetting behaviour. Sarina et al. (2012) reported that the contact angles of Al/Al_2O_3, Al/SiC and Al/graphite at 700°C are calculated to be 97°, 79°, 92° (for vitreous graphite) and 126° (single- and poly-crystal graphite), respectively. At elevated temperature both SiC and Al_2O_3 are reacted with aluminium alloying elements, resulting in formation of $MgAl_2O_4$ and Al_4C_3 brittle intermetallic phases. These brittle intermetallic phases are severely affecting the properties of the composite. To overcome these difficulties, in-situ formed TiB_2 particles is one of the major solutions to counteract wettability associated problems [7,8]. As reported by Rhee et al. the contact angle of Al on hot-pressed TiB_2 was 55° at 98% theoretical density at 840°C. Storozhenko et al. [4] reported that the NiCrBSiC alloy had good wetting properties with TiB_2 ($\theta = 34°$). Hence the wettability of Al/TiB_2 good as compared with Al/Al_2O_3, Al/SiC and Al/graphite MMCs. Low density, good thermal and electrical properties, corrosion resistance,

[1] CARE COLLEGE OF ENGINEERING, DEPARTMENT OF MECHANICAL ENGINEERING, TRICHY-620 009, TAMIL NADU, INDIA
[2] HINDUSTHAN COLLEGE OF ENGINEERING AND TECHNOLOGY, COIMBATORE – 641 032, TAMILNADU, INDIA
[3] SONA COLLEGE OF TECHNOLOGY, DEPARTMENT OF MECHANICAL ENGINEERING, SALEM – 636 005, TAMIL NADU, INDIA
[4] ANNAMALAI UNIVERSITY, DEPARTMENT OF MANUFACTURING ENGINEERING, ANNAMALAI NAGAR-608 002, TAMIL NADU, INDIA
* Corresponding author: bgkrish.mech@gmail.com

and good damping capacity make aluminium alloys one of predominant matrix materials for composite [6,7]. Fabrication of AMMCs through in-situ technique comprises synthesizing suitable reinforcements while the process itself. This method offers notable advantages over the traditional ex-situ method in terms of its capacity to produce smaller grain sizes and maintaining high thermodynamic stability [8,9]. Nowadays, many researchers have fabricated and characterise the mechanical and tribological properties of in-situ formed MMCs but, meagre work has been reported so far related to effect of secondary working and heat treatment of this composites. In spite of the fact that the stir casting technique will yield cast metal with good mechanical and tribological properties [10]. The process parameter must be chosen in such a manner to achieve defect free, good quality cast metal [5]. The material properties predominantly depend on the quality of the cast metal [9,10]. In other words, synthesized material properties generally depend on the process parameters such as reinforcement particles addition, stirring speed, stirring time, holding time, secondary working and heat treatment [7-9]. Among these parameters, reinforcement addition, secondary working and heat treatment play a vital role for deciding the final properties of composites [10]. Reinforcement particle addition has a significant role in deciding mechanical properties [11-14]. The addition of reinforcing particles into the matrix gives superior mechanical properties than base metal but beyond a certain level, it may reduce the properties. It is due to the fact that, when the addition of particles exceeds a certain volume or weight percentage, clustering or agglomeration, porosity and pin holes were formed in the cast metal resulting in defects and hence materials undergo failure [15]. The intrinsic limitations of the casting process limited the use of as-cast composites and they are exposed to secondary working followed by the heat treatment [16,17]. The morphology of the composite is generally changed during secondary working because of the distinction in the properties between the ceramic reinforcement and the ductile matrix which offer the beneficial effect to improve the final properties of the composites. In other words, the increase in mechanical properties of secondary worked materials can be attributed to the improvement of microstructural densification, interface bonding and lowering of porosity [13,15]. Moreover, selection of reinforcement is one of the key roles to decide the composite properties [16]. The reinforcement particle size, shape, and bonding strength are playing a vital role for deciding the final properties composite. Ex-situ formed SiC particles have an irregular shape and are larger in size, hence crack initiation is faster than in fine in-situ formed TiB_2 particles. This is due to the in-situ formed TiB_2 particles have micron in size and good interfacial bonding strength [12,16]. Heat treatment of particulate reinforced composite comprises solutionizing, quenching and ageing. The heat-treatment is carried out not only to improve mechanical properties, but also to remove induced stresses and structural instability [16,17].

Chidambaram et al. [19] reported that 5wt.% TiB_2 particle addition in the MMC gives better mechanical properties. Rajaravi et al. [17] investigated the hardness and tensile strength properties of Al-6wt.% TiB_2 composite and it was observed that a significant improvement of hardness and tensile strength was achieved. Many research workers in their earlier studies, the mechanical and tribological characterization of in-situ formed Al-TiB_2 MMC with less than 6wt.% of reinforcement addition and limited literatures only are reported so far related to Al-TiB_2 MMC above 6wt.%. Hence, in this investigation, an effort has been made to study the effect TiB_2 particles addition (4wt.% to 8wt.% with increment of 2wt.%) on mechanical properties of an aluminium based MMCs and compared with Al-SiC (ex-situ) MMCs. Moreover, this paper is a follow up work of the published paper [11].

2. Experimental work

The selected base metal for this investigation was wrought Aluminium 6061 alloy. The weight fraction of the individual alloying components contained in the base metal was estimated using a vacuum spectrometer (ARL, model 3460). The spectrums were obtained by igniting sparkles at various locations and estimating their compositions (TABLE 1).

The fabrication of ex-situ formed Al-SiC MMCs consist of incorporation of Silicon Carbide particles (SiC) with sizes of 22 μm and weight percentages of 4wt%, 6wt%, and 8wt% into the aluminium melt at a temperature of 720°C, whole melt was carried out by the stir casting method. The melt temperature was kept between 700 and 750°C. The current rating was kept at 20Amps. SiC powder was pre-heated at 750°C for 2 hours in a muffle furnace before being gradually added to molten aluminium. Nitrogen gas was applied to the surface of the aluminium melt at a rate of 4 litres per minute, and 1 percent Magnesium was added and mechanically stirred. The mechanical stirrer is made of mild steel, rotates at a constant speed of 300 rpm. The temperature was then kept between 710 and 730°C. Within the next 15 minutes, all of the SiC powder was completely dropped into the melt, and the stirring process was continued for an additional 10 minutes. After 25 minutes of total stirring, the 720°C melt was poured into the permanent mould and allowed to solidify at room temperature. The permanent mould was also preheated at 250°C for one hour before pouring to remove any moisture that had adhered to the mould.

The initiating materials for the fabrication of in-situ formed Al-TiB_2 MMCs are potassium hexafluoro titanate (K_2TiF_6),

TABLE 1

Chemical composition of base metal (Al6061)

Elements	Mg	Si	Mn	Fe	Cu	Zn	Ti	Cr	Al
Composition (weight %)	0.85	0.69	0.067	0.214	0.221	0.013	0.025	0.077	Remaining

potassium tetrafluoroborate (KBF_4), and wrought aluminium 6061. These halide salts were mixed in Al-TiB_2 composites with stoichiometric compositions of 4wt. percent, 6wt. percent, and 8wt. percent TiB_2. The aluminium was melted in a graphite crucible. Under normal atmospheric conditions, an electrical resistance furnace was used. The (K_2TiF_6) and (KBF_4) salts were preheated at 250°C for 30 minutes before being manually incorporated into the liquid aluminium, which was kept at 820°C. The temperature was maintained at this level for 15 minutes to allow the in-situ TiB_2 particles to form in the matrix. To prevent atmospheric contamination, nitrogen gas was supplied through a fine copper tube. The dross was skimmed off the surface of the melt twice: once before adding salts and another just before pouring. The composite melt was cast in a sand mould to fabricate the cast ingot. As-Cast Al6061 alloy and synthesized composite ingots were machined into the required number of billets (18 mm diameter and 90 mm length) from each ingot. Under laboratory conditions, billets were cold extruded with an extrusion ratio of 1.2656.

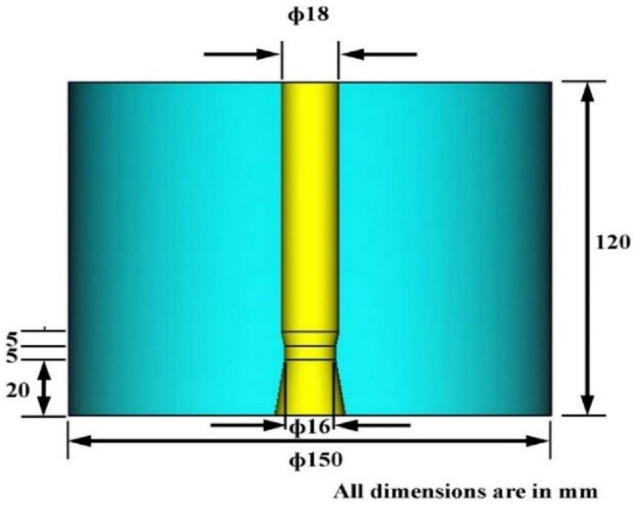

Fig. 1. Extrusion die

The schematic image of an extrusion die is shown in Fig. 1. Fig. 2(a) depicts as cast and extruded samples. All as-cast and cold extruded composite samples were shaped into the required number of tensile and hardness specimens per the ASTM E8M-16 and ASTM E18-15 standards, respectively, and then subjected to heat treatment per the ASTM B 918-01 guideline. As shown in Fig. 3, the heat treatment processes involved were solutionizing, hot bath quenching, ageing, and furnace cooling. Solutionizing

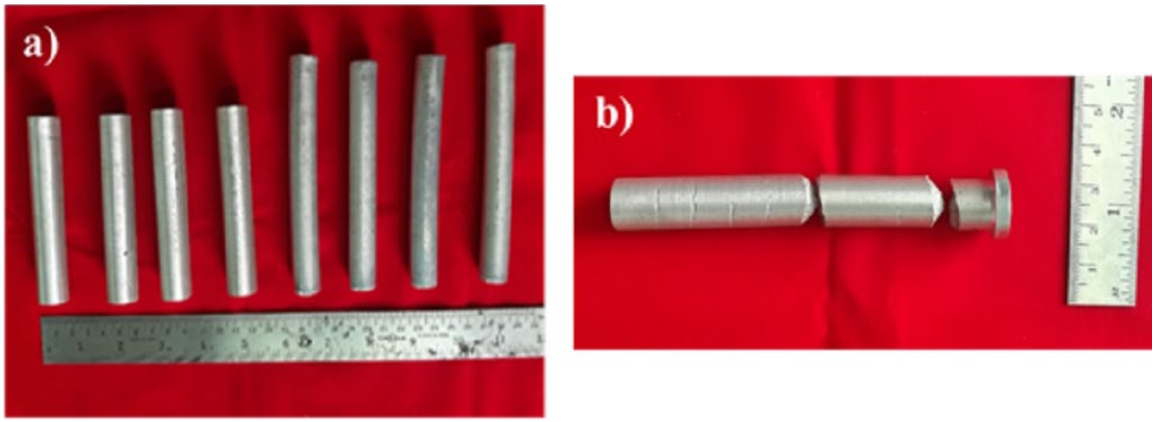

Fig. 2. Specimens a) as cast and extruded specimens & b) Cracked Al-10wt.% of TiB_2 billet

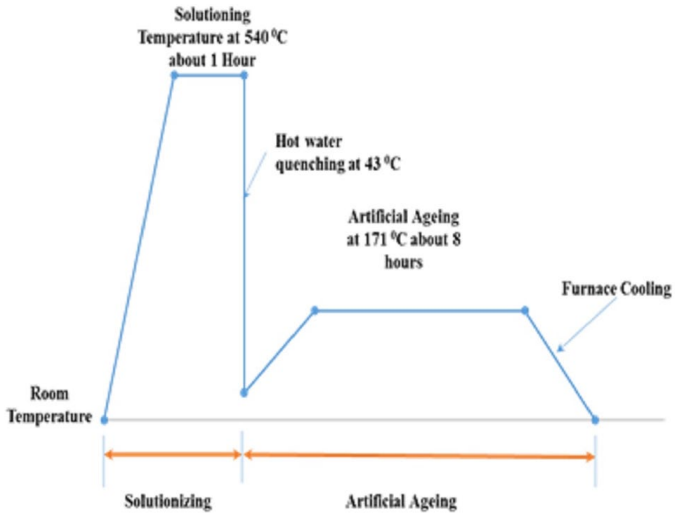

Fig. 3. Sequence of Heat treatment process as per the ASTM Standard B 918-01

was carried out for one hour at 540°C. To avoid warping of specimens, generally quenching was carried out through hot water at 43°C. Immediately, artificial ageing was performed in a muffle furnace at a temperature of 171°C for 8 hours. Temperatures were maintained to within 2°C in both solutionizing and ageing, and quench delays were kept to within 10 seconds in all cases.

Microstructural investigations were studied using a light optical microscope (Make: MEJI, Japan; Model: MIL 7100). The test samples were machined from as-cast and cold extruded composites. Specimens were polished with all sides to ensure the flatness. To ensure flatness, specimens were polished on all sides. The specimens for metallographic analyses were generally rough polished with higher-grade emery sheets before being fine polished with a series of water emery sheets. Final polish was carried out by a disc polishing machine with alumina powder. The specimens were etched according to the ASTM standard E407 with standard Keller's reagent containing 190 ml of distilled water,

5 ml of HNO_3, 3 ml of HCl and 3 ml of HF. The chemical etchants were thoroughly washed in running water. Following that, the etched samples were placed in the optical microscope to spot the macrograph. SEM (Make: JEOL, JSM-6610LV) analysis was conducted in the Scanning Electron Microscopic laboratory, Department of Manufacturing Engineering, Annamalai University, Tamilnadu.) Energy-dispersive X-ray spectroscopy (EDX) analysis is primarily useful in understanding the main microstructure, fracture analysis, boundary studies, and elements in composites. XRD and Element Mapping analysis (XRD and Element Mapping analyses were conducted in PSGTECHS COE INDUTECH Laboratory, Center of Excellence for Industrial & Home Textiles, Promoted by Ministry of Textiles – Government of INDIA.) used to identify the phases present in the fabricated MMCs.

2.1. Limiting of weight percentage of reinforcement addition

Two trial tests have been conducted on Al/10wt.% TiB_2 MMC, mechanical and microstructural characterization was analysed. The tensile strength, Elongation at fracture and hardness of the first tail is 24 MPa, 9.2% and 45 R_B respectively whereas the second trail is 23 MPa, 9.8% and 42 R_B respectively which was very poor compared to base metal as shown in Fig. 4. It is because of the formation of Al_3Ti and AlB_2 intermetallic coupled with TiB_2 particles agglomeration in aluminium matrix as shown in Fig. 5(a & b). This reduced the load carrying capacity of the composite material and propagation of crack was accelerated. When the Al-10wt.% TiB_2 composite billet was subjected to a cold extrusion process, it could not withstand the extrusion load and broke into three pieces as shown in Fig. 3(b). Hence, the percentage weight fraction of TiB_2 addition is limited within the range of 4wt.% to 8wt.%.

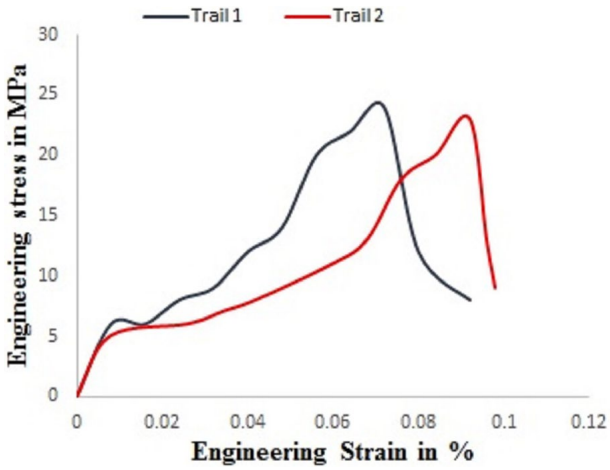

Fig. 4. stress strain curve for Al/10wt.% TiB_2 MMC

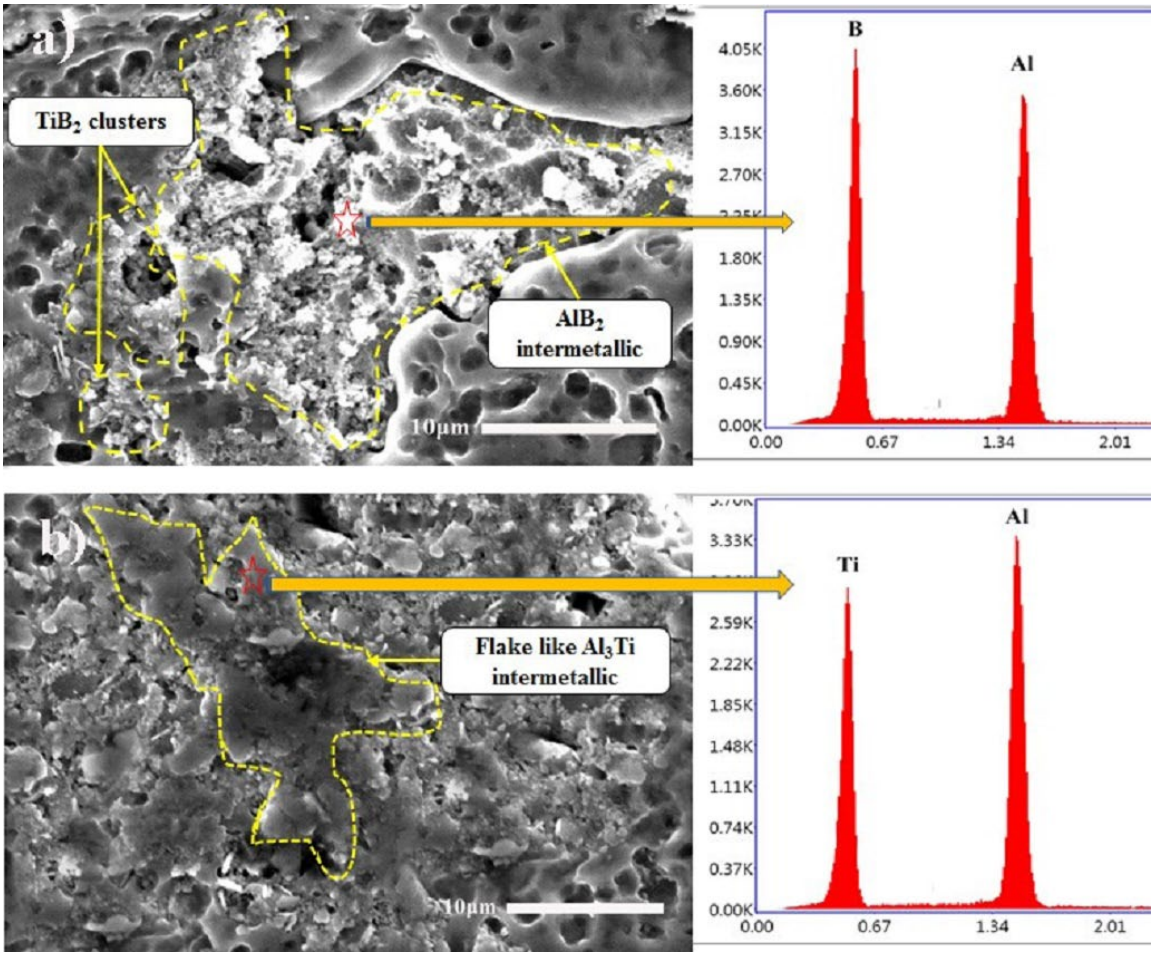

Fig. 5. SEM micrograph and EDX analysis of Al-10wt.% of TiB_2 MMC

3.1. Effect of cold extrusion on microstructure of Al-SiC MMCs (Ex-situ)

The microstructure of the cold extruded & heat-treated base metal and its Al-SiC MMCs are shown in Fig. 6. As shown in Fig. 7(b-d), the SiC particles are dispersed more homogeneously in the cold extruded composites after heat treatment. Clusters of SiC particles initially present in the as-cast condition (Fig. 6(b-d)) have completely disappeared [22]. This is because the shear stress applied during cold extrusion splits the SiC clusters and results in more homogeneous distribution. According to the Hall-Petch effect, after the cold extrusion process, aluminium grains have been reduced. The average grain size of the as-cast condition lies between 75-90 μm (Fig. 6) whereas in cold extruded condition 50-70 μm (Fig. 7). Hence, numerous aluminium grain boundaries were formed as shown in Fig. 7. These grain boundaries act as barriers to the dislocation motion hence, the mechanical properties were enhanced. As shown in Fig. 7, the presence of Mg_2Si

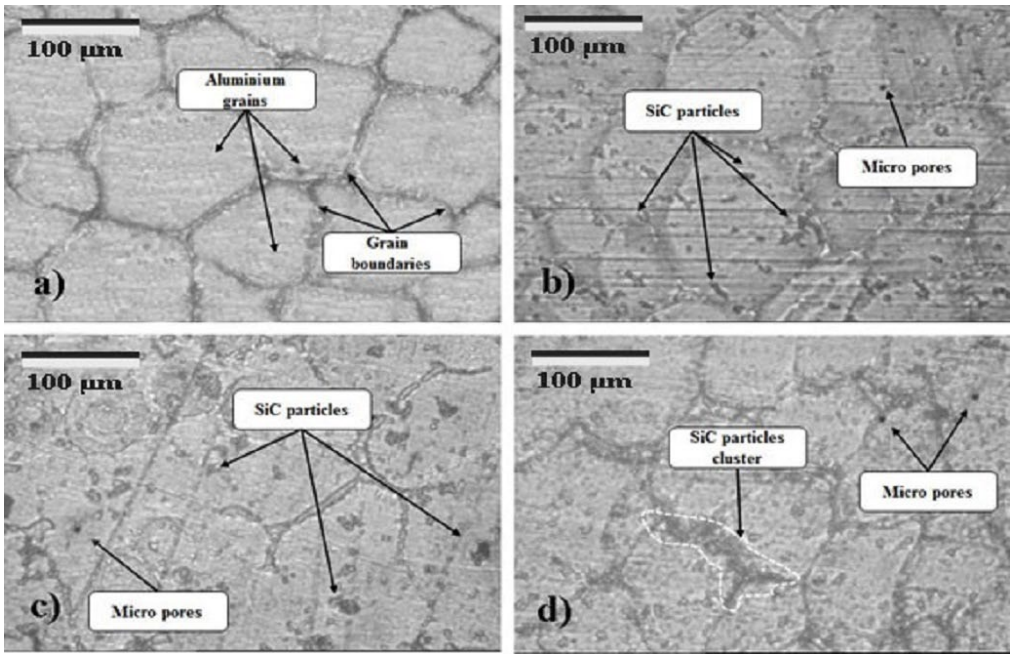

Fig. 6. Optical Microstructure of as-cast base metal & Al-SiC MMCs. a) base metal, b) Al-4wt.% SiC MMC, c) Al-6wt.% SiC MMC and d) Al-8wt.% SiC MMC

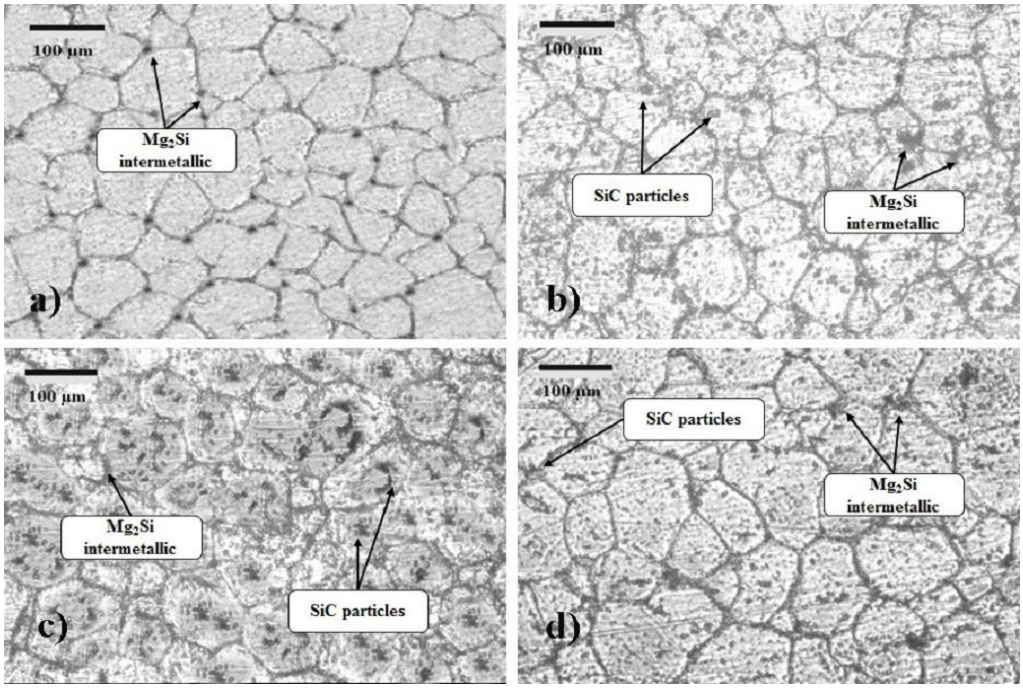

Fig. 7. Optical microstructure of cold extruded base metal & Al-SiC MMCs. a) base metal, b) Al-4wt.% SiC MMC, c) Al-6wt.% SiC MMC and d) Al-8wt.% SiC MMC

and Al_5FeSi intermetallic phases can be seen in the base metal and its composites. These intermetallic phases are, precipitated during ageing, contribute to the increase in strength of the base metal as well as composites [23]. Fig. 8(a-d) shows the SEM micrographs of base metal and its Al-SiC MMCs at cold extruded & heat-treated condition.

They reveal that the SiC particles are uniformly distributed in the aluminium matrix. The size of the SiC particles may be found smaller after extrusion and the same can be because of breakage of particles during extrusion. On the whole, the strength of the composites can be attributed to the uniformly distributed SiC particles along with Mg_2Si intermetallic phases.

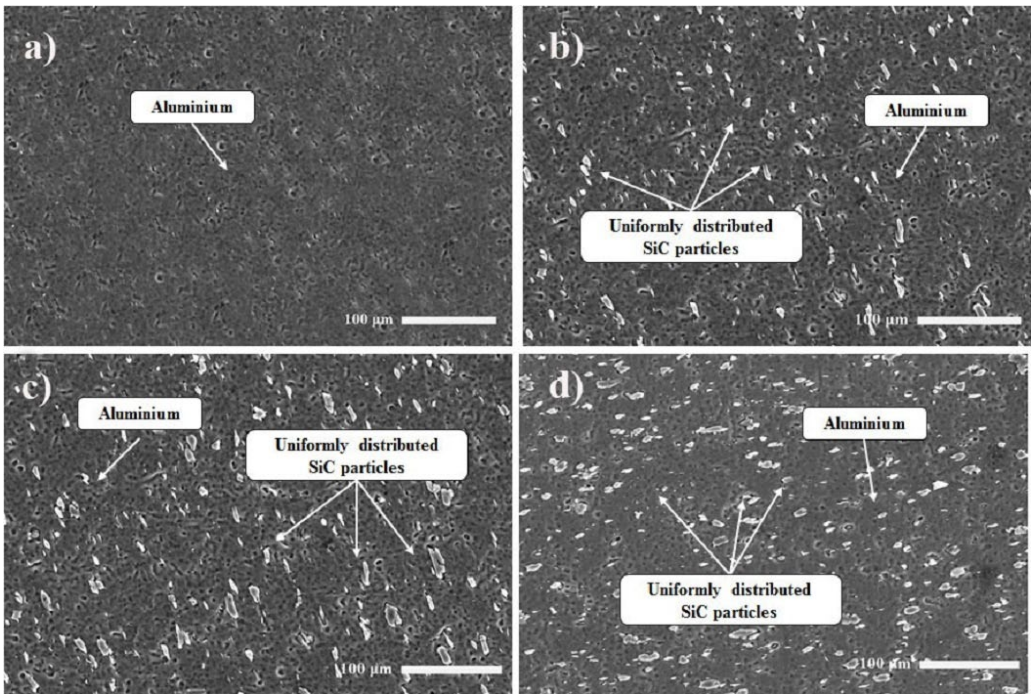

Fig. 8. SEM micrographs of cold extruded base metal & Al-SiC MMCs. a) base metal, b) Al-4wt.% SiC MMC, c) Al-6wt.% SiC MMC and d) Al-8wt.% SiC MMC

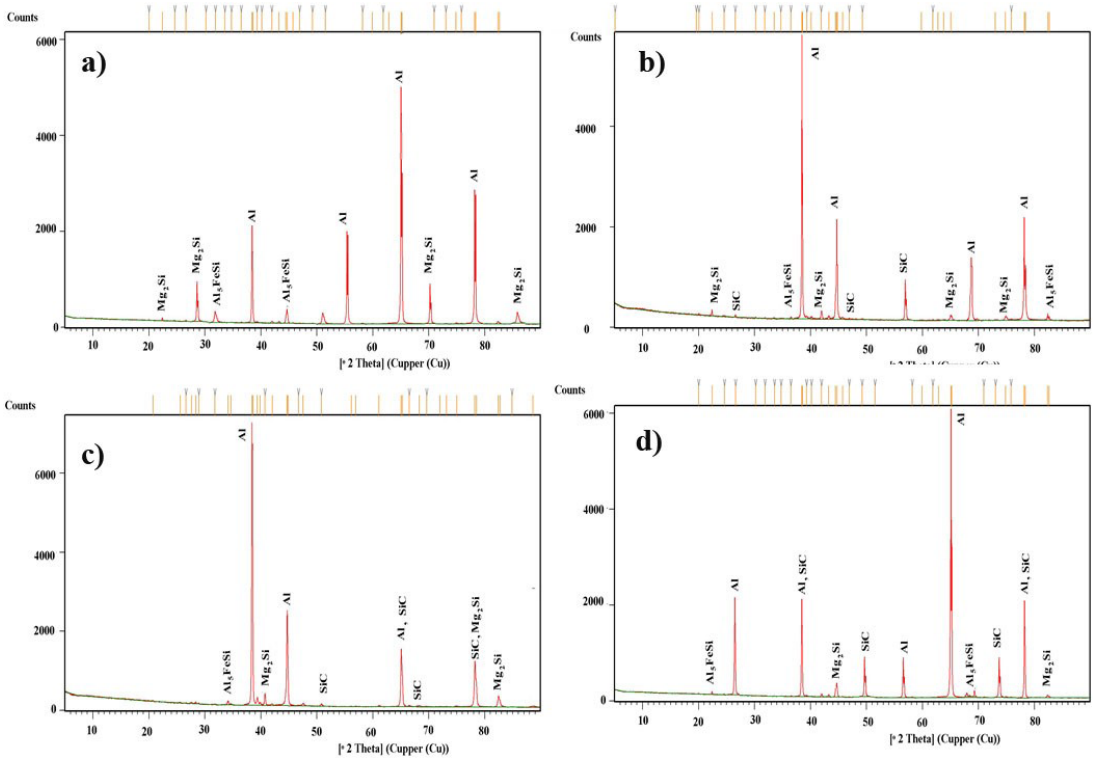

Fig. 9. XRD results of cold extruded base metal & Al-SiC MMCs. a) base metal, b) Al-4wt.% SiC MMC, c) Al-6wt.% SiC MMC and d) Al-8wt.% SiC MMC

XRD studies performed on cold extruded & heat-treated Al-SiC MMCs and base metal (Fig. 9) indicate the presence of Al, SiC, Mg_2Si and Al_5FeSi. During heat treatment, supersaturated solid solution of Mg and Si in aluminium matrix causes the formation of Mg_2Si intermetallic phase and sometimes reacts with Fe forming Al_5FeSi phase. The formation of these intermetallic phases will influence the enhancement of properties.

Moreover, the intensity of Mg_2Si peaks progressively decreases with increasing presence of hard ceramic reinforcement [24,25]. This is because, when the contents of reinforcements increase, it leads to increase in the number of particle interfaces and this affects precipitation process and hence, reduces the Mg_2Si intermetallic phases. Fig. 10 shows EDX analysis of Al-8wt.% SiC MMC, which confirms the presence of aluminium, SiC and Mg_2Si intermetallic and its alloying elements viz. Si, Mg, Cr, Fe in the cold extruded and heat-treated composites. These reinforcements and intermetallic phases are confirmed by XRD analysis in the Fig. 9.

Similar trend was noticed in the element mapping analysis as shown in Fig. 11. For Al-8wt.% SiC MMC the elemental compositions are Si-5.21%, Mg-6.52%, C-4.32%, Fe-2.01%, Cr-0.73%, and Al-81.21% and these values are very close to the EDX results. Hence, the presence of SiC particles along with Mg_2Si intermetallic phase are once again confirmed by this analysis.

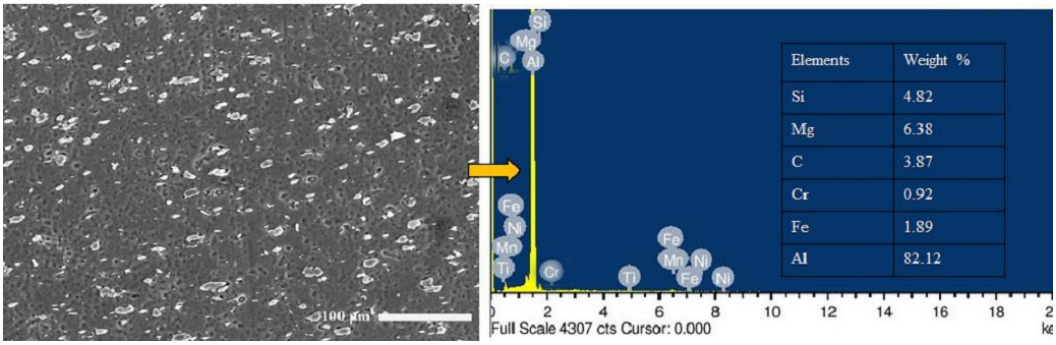

Fig. 10. EDX results of cold extruded Al-8wt.% SiC MMC

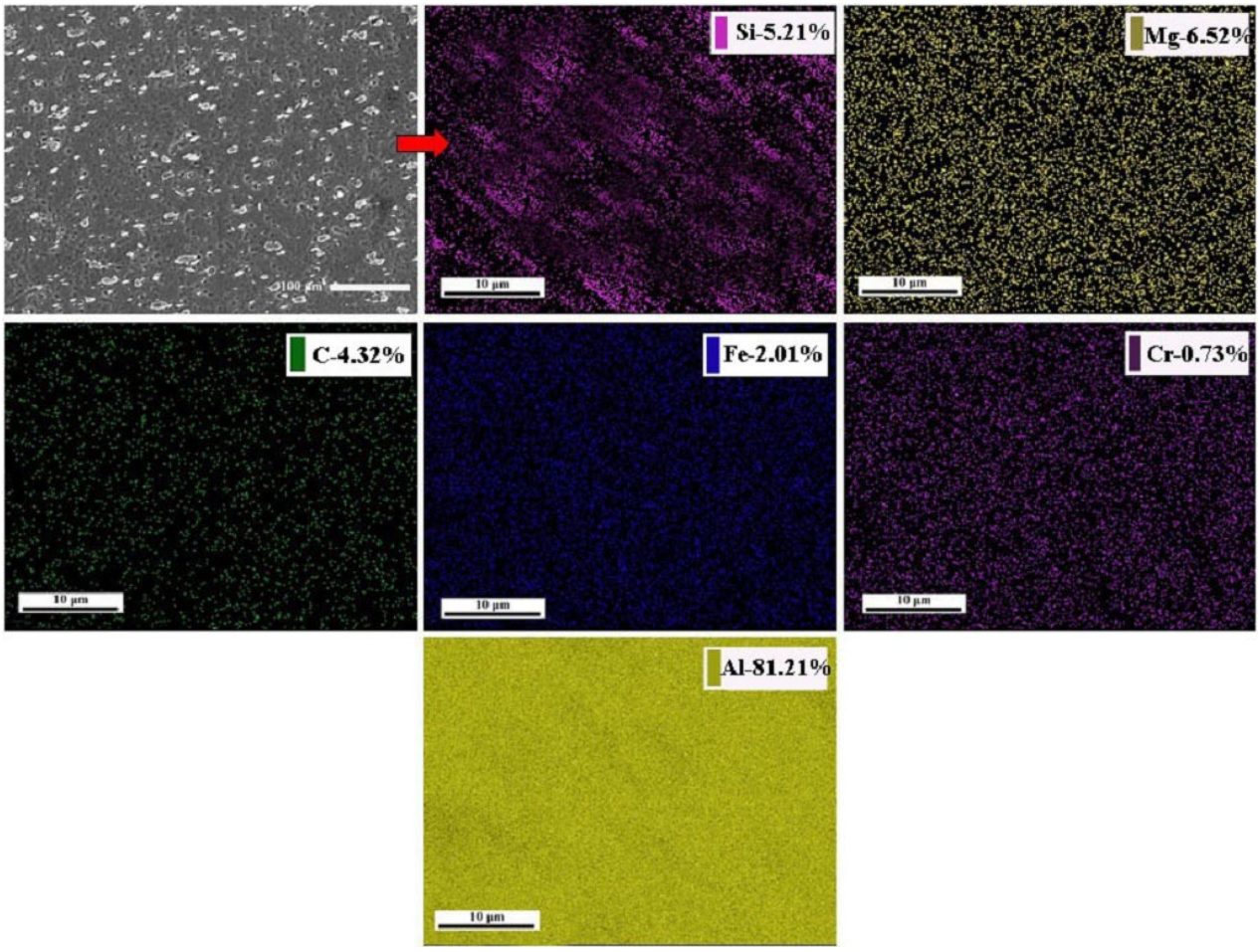

Fig. 11. Element mapping analysis of cold extruded Al-8wt.% SiC MMC

3.2. Effect of cold extrusion on macro hardness of Al-SiC MMCs

TABLE 2 shows mechanical properties of cold extruded Al-SiC MMCs. Increases in the weight percentages of SiC content can result in a significant increase in hardness. The maximum improvement of hardness of cold extruded Al-8wt.% SiC MMC over base metal is 29.85%. It is concluded that, the enhancement of hardness is mainly attributed to the content and uniform dispersion of SiC particles, microstructural densification and precipitation of fine Mg_2Si intermetallic phase. In general, when SiC particles are incorporated into a soft aluminium matrix, they resist dislocation movement, increasing the hardness of the composite. Extrusion process disburses clusters, reduces pores and improves the microstructural densification leading to increase in hardness of the composites [23,25]. Nevertheless, during heat treatment, formation of fine Mg_2Si intermetallic phases will resist the dislocation motion. The above discussed phenomenon's influences the increase in hardness of the cold extruded composites [16,17,26].

3.3. Effect of cold extrusion on tensile property of Al-SiC MMCs

The increase in tensile properties (Fig. 12) of composites is mainly governed by matrix and reinforcement material properties, as well as secondary processing. Cold extruded base metal properties such as 0.2 percent proof strength and UTS are 102 MPa and 175 MPa, respectively, whereas Al-8 wt. percent SiC composite properties are 152 MPa and 216 MPa, respectively. Cold extruded Al-8 wt. percent SiC composite improves proof strength and UTS by 0.2 percent over base metal by 49.01 percent and 23.42 percent, respectively.

The cold extruded Al-SiC MMCs have more 0.2% proof strength, UTS than that of base metal. This is because secondary working coupled with heat treatment will result in reduction of the pores and agglomeration present in the composites. Meantime, extrusion increases the fraction of aluminium grain boundaries [27]. Fine Mg_2Si intermetallic phase gets precipitated during heat treatment, playing a dominant role in dictating the final properties of composites [28]. In other words, during extrusion, densification takes place and thus increases grain boundaries resulting in low deformation during tensile load. Furthermore, the coefficient of thermal expansion mismatch between matrix

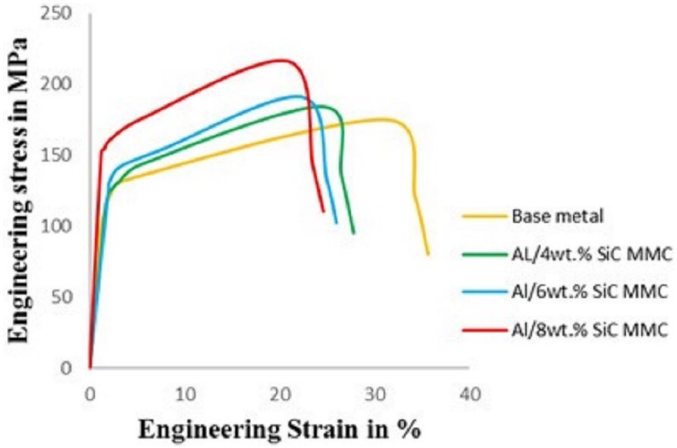

Fig. 12. Engineering stress strain curves of cold extruded base metal & Al-SiC MMCs

($23.5\times10^{-6}\,K^{-1}$) and SiC ($4.7\times10^{-6}\,K^{-1}$) results in residual plastic strain between matrix and reinforcement, increasing composite strength [27,29]. The elongation to failure decreases gradually as the fraction of ceramic particles in the matrix increases. This is due to the brittle nature of the ceramic particles, which reduces the ductility of the matrix [17,29,30].

3.4. Fractography of cold extruded Al-SiC composite

Fig. 13, reveals brittle fracture of SiC particles. Meantime, the surrounding matrix exhibits ductile shear bonds and shallow dimples confirming features of ductile rupture.

The correlation between the interfacial bonding strength and particle strength is the critical phenomenon for deciding fracture mode of the composites during tensile test. Extrusion increases the strength of the particle-matrix interfacial bonding, allowing the applied tensile load to be effectively transferred to the reinforcing phases [26,27]. However, beyond a certain point, particle fracture occurs, as evidenced by the microstructure.

4.1. Effect of cold extrusion on microstructure of Al-TiB_2 MMCs (In-situ)

The composite microstructure (Fig. 14) shows that TiB_2 particles are uniformly distributed in the matrix, along with

TABLE 2

Mechanical properties of Al-SiC MMCs for cold extruded condition

S. no	Synthesized materials	Cold Extruded condition			
		Rockwell hardness (R_B)	0.2% proof strength (MPa)	Ultimate tensile strength (MPa)	Elongation in gauge length (%)
1	Base metal	67	102	175	35.6
2	Al-4 wt.% SiC	70	112	184	27.8
3	Al-6 wt.% SiC	76	126	191	26.01
4	Al-8 wt.% SiC	87	152	216	24.6

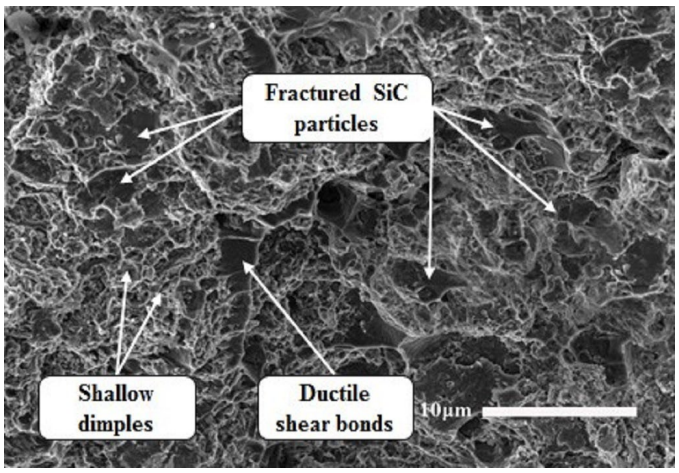

Fig. 13. Fractured surface of cold extruded Al-8wt.% SiC MMC

Mg_2Si intermetallic phases. TiB_2 particle clusters are completely eliminated by the extrusion as compared to as cast condition (Fig. 15). Moreover, due to Hall-Petch effect the aluminium grains size is considerably reduced after extrusion. Extrusion followed by heat treatment reduces pores and clusters while increasing microstructural densification, as shown in Fig. 16. Hence, numerous numbers of TiB_2 particles are more uniformly distributed in the matrix as compared to that of as-cast conditions of the same. The lack of brittle intermetallic phase (Al_3Ti) and distribution of fine equally dispersed TiB_2 particles along with Mg_2Si precipitates significantly improves composite strength and hardness [22].

The presence of Aluminium, TiB_2, in-situ by-products such as Al_3Ti & AlB_2 and intermetallic phases like Mg_2Si, Al_5FeSi are confirmed by XRD analysis as shown in Fig. 17. Fig. 17(b-d) clearly indicates Mg_2Si peaks to decrease with increase in TiB_2 peaks. This phenomenon may find to have been discussed in section 3.1.

As shown in Fig. 18, EDX analysis of Al-8wt.% TiB_2 MMC, also confirms the presence of aluminium, TiB_2 and Mg_2Si intermetallic in the cold extruded and heat-treated composites.

Similar trend can be noticed in the element mapping analysis as shown in Fig. 19. For Al-8wt.% TiB_2 MMC, Si-2.84%, Mg-4.82%, B-8.96%, Ti-4.23%, Fe-1.92%, and Al-77.23% elemental compositions can be observed and found to be very close to the EDX results.

4.2. Effect of cold extrusion on macro hardness of Al-TiB_2 MMCs

TABLE 3 shows the change in hardness of the cold extruded Al-TiB_2 MMCs as a function of TiB_2 particle addition. The cold extruded composites can be found to have superior hardness than in base metal [31]**.** The maximum hardness improvement of cold extruded Al-8wt.% TiB_2 MMC over base metal is 40.29 percent. The increase in hardness can be attributed to in-situ formed sub-micron TiB_2 particles that are distributed evenly in the matrix (Orowan strengthening mechanism). In other words, the in-situ formed TiB_2 particles have higher hardness and stiffness than base metal, which may increase their resistance to plastic deformation [32]. Also, the reduction of aluminium grain size during extrusion, increases the density of the grain boundaries significantly and this could result in increase in hardness of the composites.

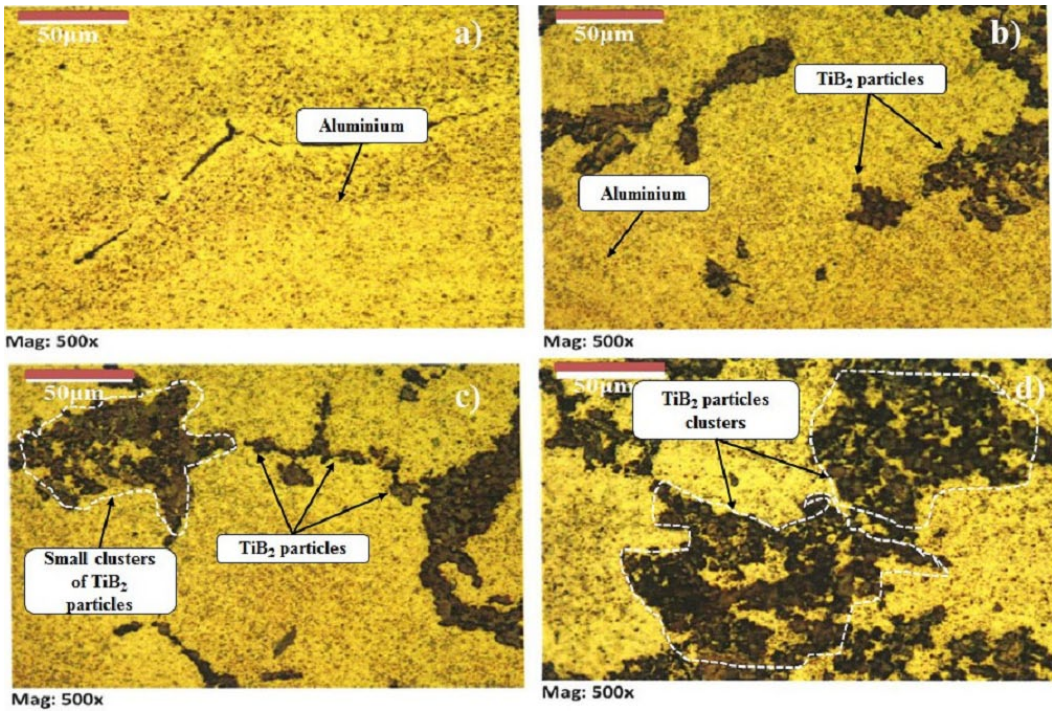

Fig. 14. Optical microstructure of as-cast base metal & Al-TiB_2 MMCs base metal, b) Al-4wt.% TiB_2 MMC, c) Al-6wt.% TiB_2 MMC and d) Al-8wt.% TiB_2 MMC

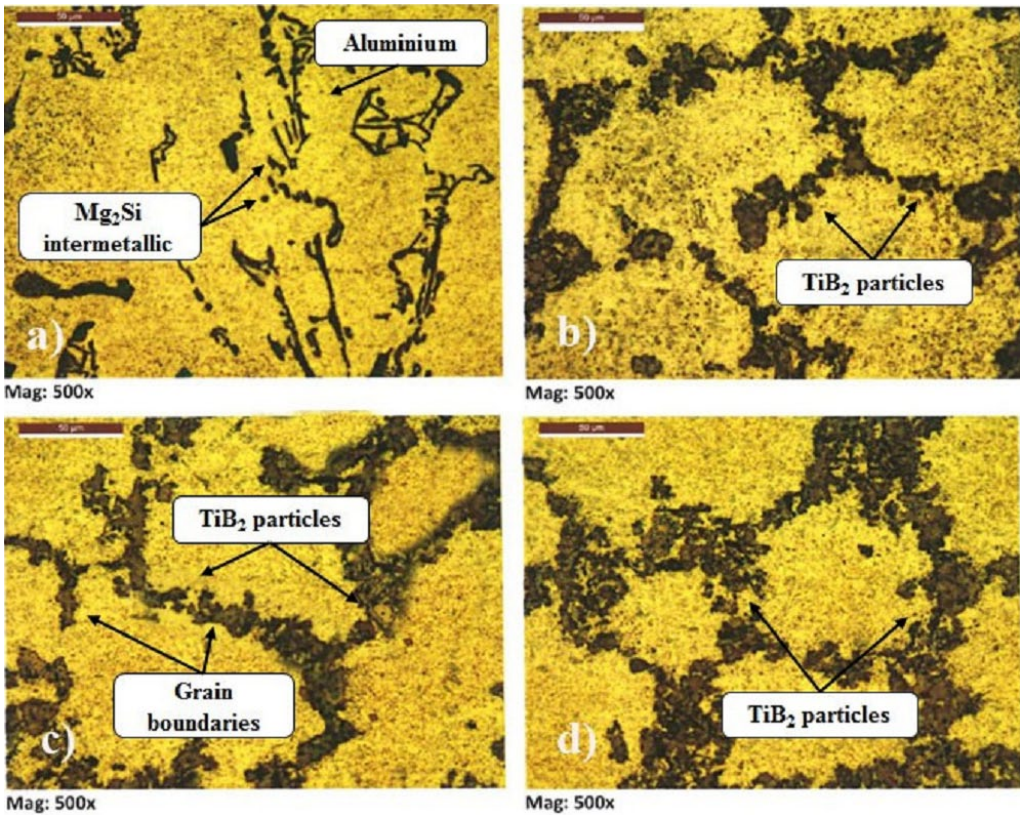

Fig. 15. Optical microstructure of cold extruded base metal & Al-TiB_2 MMCs. a) base metal, b) Al-4wt.% TiB_2 MMC, c) Al-6wt.% TiB_2 MMC and d) Al-8wt.% TiB_2 MMC

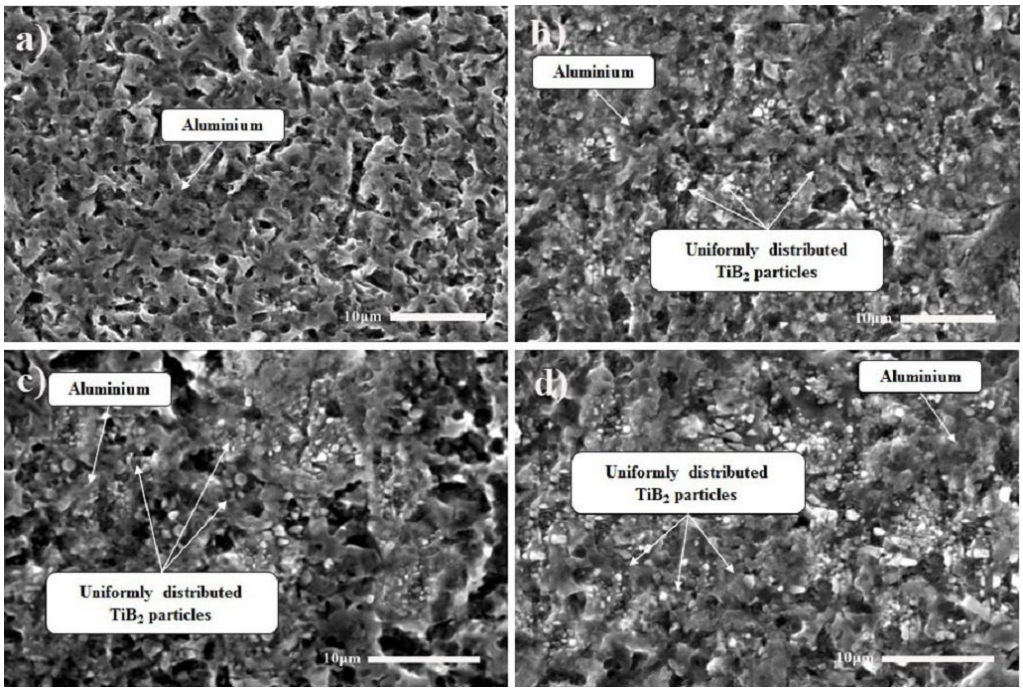

Fig. 16. SEM micrographs of cold extruded base metal & Al-TiB_2 MMCs. a) base metal, b) Al-4wt.% TiB_2 MMC, c) Al-6wt.% TiB_2 MMC and d) Al-8wt.% TiB_2 MMC

As explained by Hall-Petch, the relationship between hardness and grain size is follows: [33].

$$H = H_o + kd^{(-1/2)} \tag{4.1}$$

Where, H_o – equivalent to the friction stress, which is the intrinsic resistance of the crystal to plastic deformation, d – grain size and k – constant specific to each material. As per the above equation, it is clear that the reduction of grain size during the extrusion

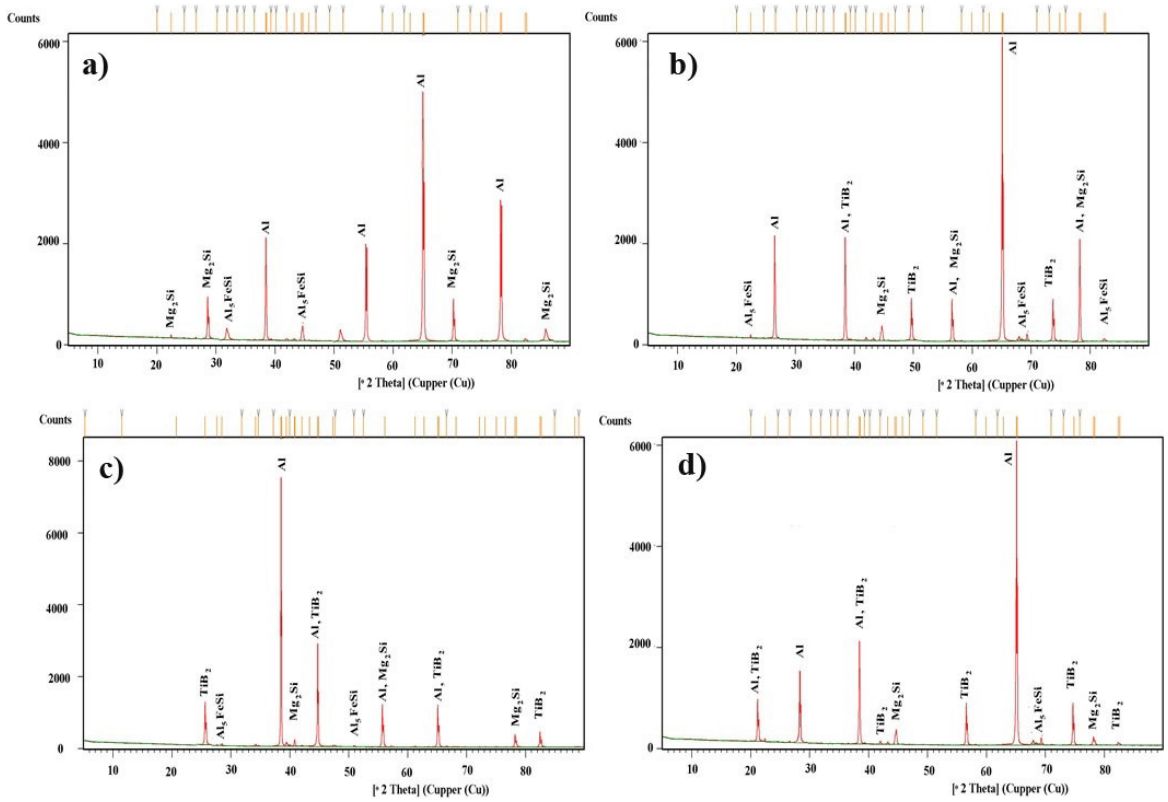

Fig. 17. XRD results of cold extruded base metal & Al-TiB_2 MMCs. a) base metal, b) Al-4wt.% TiB_2 MMC, c) Al-6wt.% TiB_2 MMC and d) Al-8wt.% TiB_2 MMC

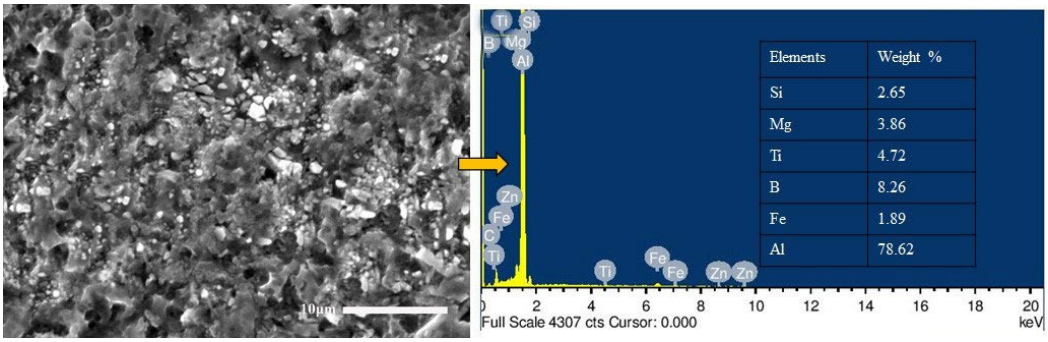

Fig. 18. EDX results of cold extruded Al-8wt.% TiB_2 MMC

process has a predominant role for increasing the hardness of the composites. The other important factors influencing the hardness of the composite are interfacial bonding strength, wetting angle and atomic nature of the interface [33,34].

4.3. Effect of cold extrusion on UTS of Al-TiB_2 MMCs

Engineering stress strain curves for cold extruded Al-TiB_2 MMCs are shown in Fig. 20. The tensile properties of Al-TiB_2 composites after cold extrusion are shown in TABLE 3. As can

TABLE 3

Mechanical properties of Al-TiB_2 MMCs for cold extruded condition

S.no	Synthesized materials	Cold Extruded condition			
		Rockwell hardness (R_B)	0.2% Proof Strength (σ_y) in MPa	Ultimate tensile strength (σ_u) in MPa	Elongation in gauge length (%)
1	Base metal	67	102	175	35.6
2	Al-4 wt.% TiB_2	74	127	224	33.4
3	Al-6 wt.% TiB_2	82	156	242	32.2
4	Al-8 wt.% TiB_2	94	192	293	28.7

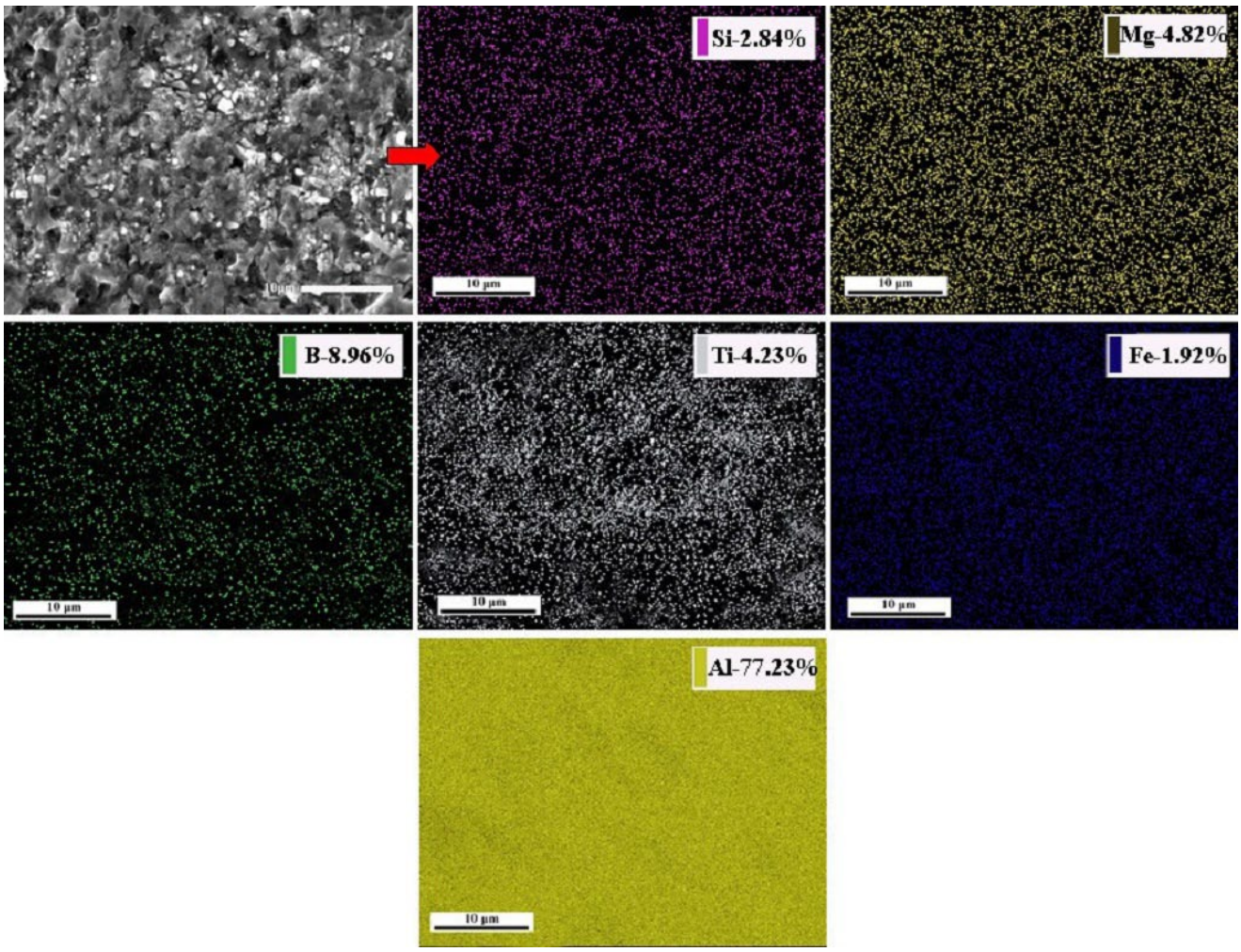

Fig. 19. Element mapping analysis of cold extruded Al-8wt.% TiB_2 MMCs

be seen, the 0.2 percent proof strength and UTS of the composites increase as the TiB_2 particle concentration increases. Cold extruded base metal properties such as 0.2 percent proof strength and UTS are 102 MPa and 175 MPa, respectively, whereas Al-8 wt. percent TiB_2 composite properties are 192 MPa and 293 MPa.

The maximum improvements in 0.2 percent proof strength and UTS of Al-8 wt. percent TiB_2 composite after cold extrusion are 88.23 percent and 67.42 percent, respectively, over base metal. The strength of the cold extruded and heat-treated composite is primarily attributed to two distinct approaches. The first is defined as the effective load transmission capacity from matrix to reinforcement, in which bonding strength and casting quality play a significant role. In this case, an In-situ formed TiB_2 particle has good bonding strength and the extrusion process increases the bonding strength. The second approach consists of three distinct mechanisms: the first mechanism is concerned with the grain refinement of the al matrix, which is accomplished by the addition of Reinforcement particles to the al matrix (Hall-Petch effect). It is understood that grain boundaries act as obstacles to dislocation motion, resulting in an increase in yield stress. TiB_2 particles restrict crystal growth in the aluminium matrix phase and enhance the fraction of grain boundary area [4]. Second mechanism entails the Orowan strengthening effect of TiB_2 particles. According to this mechanism, a large volume fraction of fine and sub-micron TiB_2 particles dispersed uniformly in the aluminium matrix would act as obstacles to dislocation motion [35]. As a result, dislocation loops form around TiB_2 particles, enhancing the stress required for further deformation. The final one is the emergence of residual plastic strain between the matrix and

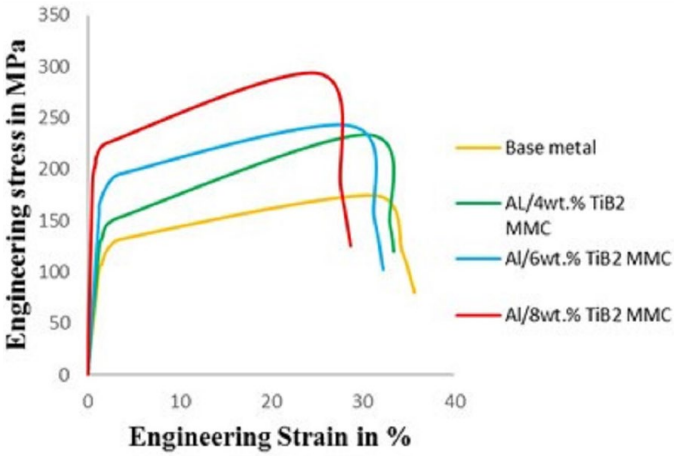

Fig. 20. Engineering stress strain curves of cold extruded base metal & Al-TiB_2 MMCs

reinforcement as a result of a thermal mismatch in the coefficient of thermal expansions, which causes an increase in dislocation density. Thus, in terms of strength increase, the aforementioned phenomena apply to the Al-TiB_2 composite [35-37]. When the elongation to failure is considered, a continuous decrease in ductility is observed as the amount of TiB_2 particles increases. Section 3.3 covered detail about why this is so.

4.4. Fractography of cold extruded Al-TiB_2 composite

As it is seen in Fig. 21, many fine and deep dimples appear on the fracture surface of cold extruded Al-8wt.% TiB_2 MMC. Moreover, it is also observed that some particles exist in some dimples, yet most of the dimples do not contain TiB_2 particles and thus it is decided that the failure of in situ composite is mainly caused by particle detachment. There is no evidence of particle fracture [38-40]. The particles and their surrounding regions are subjected to tensile load during the tensile test; the strongly embedded TiB_2 particles in the matrix are pulled out, resulting in the formation of dimples. As it is seen fig. 24, Most of the dimples are less than 5 μm in diameter and are mainly caused by in situ formed TiB_2 particles. As a result, it is concluded that the increment in mechanical properties is primarily due to TiB_2 particle pull outs. Because particle pull outs acquire more energy during deformation, they increase strength and toughness [41].

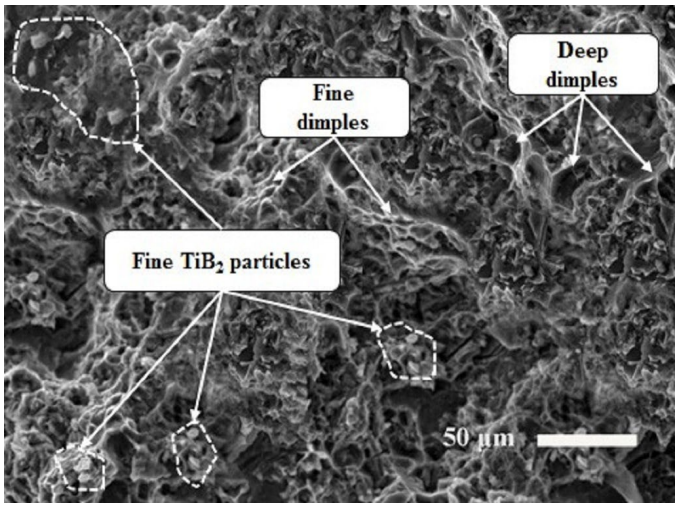

Fig. 21. Fractured surface of cold extruded & heat-treated Al-8wt.% TiB_2 MMC

5.1. Comparison of Mechanical properties of Ex-situ & In-situ formed MMCs

As observed in TABLE 4 & Fig. 22(a), In-situ formed Al-TiB_2 MMCs have significant improvements in hardness as compared to the hardness values of cold extruded Al-SiC MMCs of weight fractions of 4wt.%, 6wt.% and 8wt.% SiC. The hardness values of cold extruded Al-TiB_2 MMCs of corresponding weight fractions of TiB_2 are higher by, 5.71%, 7.89% and 8.04% respectively than Al-SiC MMCs. It is clear that the enhancements of hardness of in-situ composites over ex-situ composites are not more than 10%. It is because, during the hardness test, the localised pressure was induced directly beneath the indenter surface to endorse the majority of the load. As a result, the stress field directly beneath the indenter is widely compressive with the matrix when subjected to severe triaxial pressure.

Both the SiC and TiB_2 particles can withstand the compressive load effectively. The deformation caused by the indentation pressure is accommodated by the plastic flow of the matrix between the particles, and the particles are driven into the matrix material [40,46].

As a result, the hardness of the composites increases as the weight fraction of SiC particles increases. From the above discussion, both the SiC and TiB_2 particles are almost equally effective in resisting the indentation load during hardness test. Hence the difference is much less than other properties.

Variation of 0.2% proof strength corresponding to varying wt.% of reinforcement addition with different working conditions are shown in TABLE 4 & Fig. 22(b). It is concluded that, in-situ composites have a higher 0.2% proof strength. As compared to the 0.2% proof strength of cold extruded Al-SiC MMCs of weight fractions of 4wt.%, 6wt.% and 8wt.% SiC, the 0.2% proof strength of cold extruded Al-TiB_2 MMCs of corresponding weight fractions of TiB_2 are higher by, 13.39%, 23.80% and 26.31% respectively.

Two approaches can be used to increase the 0.2 percent proof strength of aluminum-based in-situ composites. First approach involves two phenomenons, one is based on the efficient load transfer capacity from matrix to reinforcement, in which bonding strength and casting quality have played a significant role and the second is based on the effect of TiB_2 particles on aluminium matrix yield strength. The second approach includes three distinct mechanisms: the first mechanism is matrix grain refinement, which is accomplished by incorporating TiB_2 par-

TABLE 4

Comparison of Mechanical properties of cold extruded Ex-situ & In-situ formed MMCs

Mechanical properties of cold extruded Ex-situ & In-situ formed MMCs									
S.no	Materials	Rockwell hardness (R_B)		0.2% Proof Strength (σ_y) in MPa		Ultimate tensile strength (σ_u) in MPa		Elongation in gauge length (%)	
		Al-SiC	Al-TiB_2	Al-SiC	Al-TiB_2	Al-SiC	Al-TiB_2	Al-SiC	Al-TiB_2
1	Base metal	67	67	102	102	175	175	35.6	35.6
2	4wt.%	70	74	112	127	184	224	27.8	33.4
3	6wt.%	76	82	126	156	191	242	26.01	32.2
4	8wt.%	87	94	152	192	216	293	24.6	28.7

ticles into the matrix material (Hall-Petch effect). The grain boundaries are believed to act as barriers to dislocation movement [42,43]. As a result, 0.2 proof strength is increased. TiB_2 particles limit the grain growth of the aluminium matrix phase and greatly increase the grain boundary. Furthermore, during cold extrusion, composites are subjected to serious compressive stress along the transverse direction, resulting in significantly reduced grain size and an increase in 0.2 percent proof strength [44,45]. According to the Second mechanism, a higher volume fraction of fine and sub-micron TiB_2 particles distributed uniformly in the aluminium matrix would act as obstacles to dislocation motion. As a result, dislocation loops form around TiB_2 particles, increasing the stress required for further deformation [42,46]. Third is the establishment of residual plastic strain between the matrix and reinforcement as a result of a thermal mismatch in thermal expansion coefficients, resulting in an increase in dislocation density [43-46]. The effect of heat treatment on 0.2% proof strength, is mainly attributed by the preeminent holding temperature (around 540°C at one hour) of the composite during the solutionizing period. It leads to an increase in dislocation density due to imbalance in coefficients of thermal expansion between the aluminium matrix (23.5×10^{-6} K^{-1}) and the TiB_2 reinforcement (7×10^{-6} K^{-1}) at the interface during water quenching. This effect is a major contributor to the increased strength of composites. Thus, in terms of strength increase, the aforementioned phenomena apply to the Al-TiB_2 composite.

The Ultimate tensile strength of ex-situ & in-situ formed composites are shown TABLE 4 & Fig. 22(c). As compared to the UTS of as-cast Al-SiC MMCs of weight fractions of 4wt.%, 6wt.% and 8wt.% SiC, the UTS of as-cast Al-TiB_2 MMCs of corresponding weight fractions of TiB_2 are higher by, 21.73%, 26.70% and 35.64% respectively. In-situ formed MMCs have higher UTS than ex-situ MMCs. This is because TiB_2 is finer and more regular in shape than SiC. It is embedded into a soft molten aluminum, resulting in increased deformation resistance and, as a result, an improved UTS of the composite material. The modification and fineness of the reinforcement also play an important role in deciding composite material strength. Fine and clear interfacial bonding is achieved through the exothermic reaction that occurs during in-situ composite fabrication. Likewise, manufacturing technique and casting soundness strengthen the composite significantly [42-45]. The load transfer capability from matrix to reinforcement is enhanced by the reaction free interface. The strength of the composite increases as the matrix's load transfer capability to the reinforcement increases [43]. It is noted that the homogeneity of TiB_2 particles, associated with a reaction-free interface between matrix and reinforcement, allows for effective load transfer from matrix to reinforcement. As a result, the strength of the composites improves.

Chidambaram et al. (2019) produced AA6061-5wt. %TiB_2 in-situ metal matrix composite subjected to equal channel angular pressing and reported that, the AA6061 alloy's yield strength is 105 MPa, ultimate strength is 123 MPa, and elongation to failure is 27%. Rajaravi et al. (2019) Fabricated Aluminium based in-situ formed 6wt.% TiB_2 composites with different pouring temperatures such as 800° C, 820° C and 840° C and maximum obtained UTS was 165 MPa. In the present work remarkable improvement in UTS has been obtained 293 by the cold extruded composite. In general, the strength of an aluminium alloy is explained by the Hall-Petch hardening mechanism and the size of the -Al grain. Particle size in the aluminium matrix is demonstrated by Orowan mechanism and strengthening of the composite is explained through solid solution hardening of the composite. The ageing kinetics are improved by the amount of TiB_2 reinforcement particles [38,46].

The variations of elongation to failure of Ex-situ & In-situ formed MMCs are shown in TABLE 4 & Fig. 22(d). It is evident that the values of elongation to failure of in-situ formed composites have consistent increment over ex-situ MMCs. In general, in-situ formed composites retain their ductility better than ex-situ composites. This is due to the particle size, shape, and bonding strength of the TiB_2 particles. Whereas, SiC particles have an irregular shape and are larger in size, hence crack initiation is faster than in fine in-situ formed TiB_2 particles. During the tensile test, the particles and their surrounding regions are subjected to tensile load; the strongly incorporated TiB_2 particles in the matrix are pulled out, resulting in dimple formation. As it is seen Fig. 21, Most of the dimples are less than 5 μm in diameter and are mainly caused by in situ formed TiB_2 particles. As a result, it is concluded that the improvement in mechanical properties can be attributed primarily to TiB_2 particle pull outs.

Furthermore, the pull-out particles absorb energy during deformation, increasing the ductility and toughness of the in-situ composites [40,42,46].

5. Conclusion

The effect of cold extrusion on microstructure and mechanical properties are concluded below:

- The microstructure revealed that the presence of Mg_2Si precipitation, the precipitation of Mg_2Si phase from the supersaturated solid solution of Mg and Si in the Aluminium matrix caused by the aging process. The presence of reinforcement particles such SiC and TiB_2 along with intermetallic phases Mg_2Si and Al_5FeSi are confirmed by EDX, XRD and Element Mapping analyses.
- Cold extruded Al-8 wt.% SiC composite properties such as hardness, 0.2% proof strength and UTS are 87 R_B, 152 MPa, 216 MPa respectively. Whereas, for Al-8 wt.% TiB_2 composite the corresponding properties are 94 R_B, 192 MPa, 293 MPa. The improvements of hardness, 0.2% proof strength and UTS of cold extruded Al-8 wt.% SiC composite over base metal are 29.85%, 49.01% and 23.42% respectively. Whereas, for Al-8 wt.% TiB_2 composite the corresponding improvements are 40.29%, 88.23% and 67.42%.
- As compared to Al-SiC composites, the maximum improvements of Al-8 wt.% TiB_2 composite properties such as hardness, 0.2% proof strength and ultimate tensile strength are 8.04%, 26.31% and 35.64% respectively.

Acknowledgements

The authors would like to thank the Department of Manufacturing Engineering at Annamalai University and the University Grant Commission (UGC)-RGNF in New Delhi, India for their assistance with this research.

REFERENCES

[1] H. Liu, B.G. Falzon, S. Li, W. Tan, J. Liu, H. Chai, B.R.K. Blackman, J.P. Dear, Compos. Struct. **1** (213), 108-17 (2019).

[2] J.P. Oliveira, K. Ponder, E. Brizes, T. Abke, P. Edwards, A.J. Ramirez, J. Mater. Process. Technol. **273**, 116192. (2019).

[3] A.R. Kennedy, S.M. Wyatt, Compos. Sci. Technol. **60** (2), 307-14 (2000).

[4] M. Storozhenko, O. Umanskyi, V. Krasovskyy, M. Antonov, O. Terentjev, J. Alloys Compd**. 778**, 15-22, (2019).

[5] S.K. Rhee, J. Am. Ceram. Soc. **53** (7), 386 (1970).

[6] Z. Wang, J.P. Oliveira, Z. Zeng, X. Bu, B. Peng, X Shao, Opt. Laser Technol. **111**, 58-65 (2019).

[7] W. Ke, X. Bu, J.P Oliveira, W. Xu, Z. Wang, Z. Zeng, Opt. Laser Technol. **133**, 106540 (2021).

[8] S.D. Kumar, M. Ravichandran, A. Jeevika, B. Stalin, C. Kailasanathan, A. Karthick, Ceram. Int. **47** (9), 12951-62 (2021).

[9] A. Chidambaram, S. Balasivanandha Prabu, K.A. Padmanabhan, Mater. Sci. Eng. A. **759**, 762-9 (2019).

[10] C. Rajaravi, B. Gobalakrishnan, P.R. Lakshminarayanan, J. Mech. Behav. Mater. **28**, (1) 162-168 (2019).

[11] B. Gobalakrishnan, C. Rajaravi, G. Udhayakumar, P.R. Lakshminarayanan, Met. Mater. Int. **27** (9), 3695-708 (2021).

[12] Sheelwant, Amar, Sunil Dutta, Kartheek S.M. Sonti, Suresh Kumar Reddy Narala, Mater. Manuf. Process 1-11 (2021).

[13] G.V. Kumar, D.G. Reddy, C.V. Reddy, C. Sriteja, R. Pramod, Mater. Perform. Charact. **9** (1), 139-150 (2020).

[14] A. Saxena, M. Indriyati, Rajveer, P. Biswas, H.R. Kotadia, S. Das, Mater. Sci. Technol. **35** (8), 953-961 (2019).

[15] Y. Ma, A. Addad, G. Ji, M.X. Zhang, W. Lefebvre, Z. Chen, V. Ji, Acta Mater. **185**, 287-299 (2020).

[16] L. Singh, B. Singh, K.K. Saxena, Adv. Mater. Process. Technol. **6** (2), 441-457 (2020).

[17] N. Gangil, A.N Siddiquee, S. Maheshwari, J. Alloys Compd. **715**, 91-104 (2017).

[18] P. Sadagopan, N.H. Karthi, J.P. Kumar, Int. J. Adv. Manuf. Technol. **94** (1-4), 1461-75 (2018).

[19] K. Mahadevan, K. Raghukandan, T. Senthilvelan, B.C. Pai, U.T.S. Pillai, J. Mater. Process. Technol. **171** (2), 314-8 (2006).

[20] T. Parameshwaranpillai, P.R. Lakshminarayanan, B. Nageswara Rao, Mater. Des. **31** (6), 2987-93 (2010).

[21] A. Bahrami, A. Razaghian, M. Emamy, R. Khorshidi, Mater. Des. (1980-2015). **36**, 323-30 (2012).

[22] S.B. Hassan, O. Aponbiede, V.S. Aigbodion, J. Alloys Compd. **466** (1-2), 268-72 (2008).

[23] M. Emamy, H.J. Nodooshan, A. Malekan. Mater. Des. **32** (8-9), 4559-66 (2011).

[24] A. Mandal, M. Chakraborty, B.S. Murty, Mater. Sci. Eng. A. **489** (1-2), 220-6 (2008).

[25] B. Gobalakrishnan, P.R. Lakshminarayanan, R. Varahamoorthi, Mater. Test. **60** (12), 1221-4 (2018).

[26] Y.M. Youssef, R.J. Dashwood, P.D. Lee, Mater. Sci. Eng. A. **391** (1-2), 427-32 (2005).

[27] H. Ghandvar, M.H. Idris, N. Ahmad, J. Alloys Compd. **1** (751), 370-90 (2018).

[28] A.M. Samuel, H. Liu, F.H. Samuel, J. Mater. Sci. **28** (24), 6785-98 (1993).

[29] J.M. Akhgar, A. Mirjalili, S. Serajzadeh, J. Mater.: Des. Appl. **225** (1), 22-31 (2011).

[30] A. Bolouri, Y.P. Jeon, C.G. Kang. Int. J. Adv. Manuf. Technol. **70** (9-12), 2139-49. (2014).

[31] R. Zamani, H. Mirzadeh, M. Emamy, Mater. Sci. Eng. A. **30** (726), 10-7 (2018).

[32] M. Emamy, M. Mahta, J. Rasizadeh, J. Compos. Sci. Technol. **66** (7-8), 1063-6 (2006).

[33] Y. Pazhouhanfar B. Eghbali, Mater. Sci. Eng. A. **5** (710), 172-80 (2018).

[34] A. Changizi, A. Kalkanli, N. Sevinc, J. Alloys Compd. **509** (2), 237-40 (2011).

[35] J. Geng, G. Liu, F. Wang, T. Hong, C. Xia, M. Wang, D. Chen, N. Ma, H. Wang, Mater. Sci. Eng. A. **27** (687), 131-40 (2017).

[36] M. Sobhani, A. Mirhabibi, H. Arabi, R.M.D. Brydson, Mater. Sci. Eng. A. **10** (577), 16-22 (2013).

[37] N. Kumar, G. Gautam, R. Kumar, G. Anita, M. Sunil, Inst. Eng. (India) Metall. Mater. Eng. Div. **97** (2), 233-53 (2016).

[38] N. Soltani, H.R. Jafari Nodooshan, A. Bahrami, M.I. Pech-Canul, W. Liu, G. Wu, Mater. Des. **1** (53), 774-81 (2014).

[39] A. Razaghian, A. Bahrami, M. Emamy, Mater. Sci. Eng. A. **1 (**15), 532:346-53 (2012).

[40] Z.G. Wang, C.P. Li, H.Y. Wang, X. Zhu, M. Wu, Q.C Jiang, Powder Metall. **59** (4), 236-41 (2016).

[41] R.K. Goswami, R. Sikand, A. Dhar, O.P. Grover, U.C. Jindal, A.K. Gupta, Mater. Sci. Technol. **15** (4), 443-9 (1999).

[42] K. Sivaprasad, S.P.K. Babu, S. Natarajan, R. Narayanasamy, B.A. Kumar, G. Dinesh, Mater. Sci. Eng. A. **498** (1-2), 495-500 (2008).

[43] C. Mallikarjuna, S.M. Shashidhara, U.S. Mallik, K.I. Parashivamurthy, Mater. Des. **32** (6), 3554-9 (2011).

[44] H. Wang, H. Zhang, Z. Cui, Z. Chen, D. Chen, H. Wang, Mater. Sci. Eng. A. **9** (764), 138263 (2019).

[45] S.L. Pramod, S.R. Bakshi, B.S. Murty, J. Mater. Eng. Perform. **24** (6), 2185-207 (2015).

[46] A. Radha, K.R. Vijayakumar, Mater. Today: Proc. **3** (6), 2247-53 (2016).